5-2014

Effects of Instrumentation on Dental Microwear Textures: Reanalysis and Augmentation of an Early Hominin Sample

Anna Jacquelyn Ragni
University of Arkansas, Fayetteville

Effects of Instrumentation on Dental Microwear Textures: Reanalysis and Augmentation of an Early Hominin Sample

Effects of Instrumentation on Dental Microwear Textures: Reanalysis and Augmentation of an Early Hominin Sample

A thesis submitted in partial fulfillment
of the requirements for the degree of
Master of Arts in Anthropology

by

Anna Ragni
Hendrix College
Bachelor of Arts in Anthropology, 2012

May 2014
University of Arkansas

This thesis is approved for recommendation to the Graduate Council.

_____
Dr. Peter Ungar
Thesis Director

_____
Dr. Joseph Plavcan
Committee Member

_____
Dr. Jerome Rose
Committee Member

ABSTRACT

Dental microwear texture analysis has been refined to a methodology relying upon scanning confocal microscopy for its advantages of repeatability and standardized quantification. A new instrument, the Plμ Neox (Sensofar Corp.) confocal profiler recently entered the market, sparking questions among dental anthropologists related to the advantages and efficacy of this new technology, which has better resolution and lighting properties than previously available white-lighted based confocal profilers. This thesis reports on three complementary studies that set out to evaluate the comparability of the Plμ Neox to the Plμ Standard system and assess its ability to distinguish primates on the basis of their microwear patterning. The first study examines a sample of hominin molars (*Australopithecus africanus* and *Paranthropus robustus*) for comparison with data previously scanned and analyzed on the University of Arkansas' Plμ Standard confocal microscope (Scott et al., 2005). The second study expands the sample of early hominins to determine whether an enlarged sample of *A. africanus* continues to show significant texture separation from *P. robustus*. And the third study examines extant primate microwear textures of pitheciids with known dietary differences to determine whether documented food-choice trends are reflected in microwear patterning obtained using the Plμ Neox. Examining pitheciine molar facets in the past was not possible because of their small size. The new instrument provides higher resolution (0.11 μm with a 150x objective compared to 0.18 μm at 100x on the Plμ Standard confocal), with a smaller work envelop for a comparable number of sampled points for texture analysis. Results of the first study generally correspond to the original texture analysis of 2005, and the expanded dataset in the second study shows increased variance but the same pattern of differences for *A. africanus* compared with *P. robustus*. The third study finds that the Plμ Neox is capable of parsing broad diet-related differences in microwear textures among the pitheciids, indicating that the new instrument may become an effective instrument for the quantitative characterization and comparison of dental microwear textures to be utilized in laboratories around the world.

ACKNOWLEDGEMENTS

Study III of this thesis was funded by the Leakey Foundation, with special thanks to the curators of the American Museum of Natural History in New York, The National Museum of Natural History in Washington DC, and Goeldi Museum in Belém for access to specimens in their care.

Thank you to Dr. Peter Ungar for your patience, specialized tutorials, and guidance throughout the course of this project. Thank you for giving me this amazing thesis topic and the opportunity to specialize in one of the most important time periods of hominin history with a brand new piece of equipment! I am forever grateful.

Thank you to Dr. Mark Teaford for sending me specimens when we could not find them in our own lab. Your generosity and patience were not unnoticed.

Thank you to Dr. Fred Grine for pre-screening several specimens and providing ample sources for specimen identification. You efforts made this project much more efficient.

Thank you to the Sensofar team in Spain for answering my endless stream of questions about the Plμ Neox confocal profiler. My ability to operate and adjust the Neox confocal profiler is a result of your cooperation, attentiveness, and willingness to help.

Thank you to my fellow lab mates who provided a supportive and challenging environment throughout this process. Your words of wisdom will not be forgotten, and good luck as you continue your respective journeys.

And thank you to my committee members for educating me throughout this process in the fields of dental anthropology and quantitative morphometrics.

DEDICATION

This thesis is dedicated to all who encouraged me along the way: to those who inspired me to stay the extra hours in an abandoned basement, and to those who gave me a reason to take a break.

TABLE OF CONTENTS

I. INTRODUCTION……...……1

II. STUDY I……1

Background: Australopith Dietary Models……...1

Contextual……2

Morphological……...3

Dental Microwear……....4

Materials and Methods……6

III. STUDY II……..…10

Background: Australopith Dietary Models…… ……....11

Materials and Methods……..... ……...11

IV. STUDY III……..……11

Background: Pitheciiid Diets……...…11

Materials and Methods……..…13

V. RESULTS……..13

Study I……...13

Study II……..16

Study III……18

VI. DISCUSSION……...…22

Study I, II, and III……...……..22

VII. CONCLUSIONS……24

VIII. APPENDIX A……26

Using the 100x Objective……...…26

Using the 150x Objective……..……26

IX. APPENDIX B……..……27

X. REFERENCES CITED……32

INTRODUCTION

Dental microwear texture analysis, in combination with scale-sensitive fractal analysis, requires digital renderings of a tooth's surface (obtained with a white-light or blue-light scanning confocal profiler) and provides repeatable analyses of dental measurements correlated to diet. The Ungar Lab at the University of Arkansas recently acquired a new instrument capable of creating more detailed 3D-surfaces. This new confocal microscope, called the Plμ Neox (Sensofar Corp.) confocal profiler, is an emerging standard in the field and can potentially discriminate between more similar diets than our Plμ Standard machine given its increased resolution and improved optical and lighting characteristics. First, though, the Neox must be tested for comparability with the Plμ Standard.

The purpose of this research is to determine the comparability of two confocal microscopes separated by nearly ten years of technology, and was completed in three studies. Study I is a comparison of results from the new confocal microscope to those from a 2005 study (Scott et al.), which established the Plμ Standard as the new discipline standard at the time. The goal of this study is to establish if a possible significant correlation can be made between surface textures for a sample analyzed using both machines. Upon comparing the data from two different machines, a new sample of as yet unanalyzed (for microwear) *Australopithecus africanus* specimens is included, with the goal of determining whether the results of the 2005 study would hold when tripling the sample of this species. Study III evaluates the efficacy of the new confocal for quantifying the diets of extant primates, the pithecoids, at an even higher resolution, yielding finer insight into their known dietary behaviors. The goal of the third study is to quantify significant differences in the diets of pitheciid taxa, which have been documented by primatologists.

STUDY I

Background: Australopith Dietary Models

The diet of early hominins has been a topic of scholarship and debate since their fossil record was uncovered nearly a century ago. These hypotheses may be divided into reasoning stemming from contextual, morphological, and dental microwear evidence.

Contextual

Dart (1940; 1948; 1949; 1953) reconstructed A. africanus as a predator based on faunal cave remains, including numerous hindlimbs, bone breakages signifying osteodontokeratic culture and dark stains suggesting fire (for food preparation). He considered this evidence to imply *A. africanus* was a "killer ape" (Dart, 1926; 1957). The holes found in fellow australopith crania were reasoned to be evidence of violence resulting from projectile weapons or assault.

These findings were later contested (Brain, 1970; 1981). The bone piles were argued to be hyena accumulations, the bone breaks said to match leopard kill patterns, and the dark markings on the floor were argued to be stains from mining explosions, discrediting the original argument for predation. Leopard canines fit perfectly into the holes of the skull seen in multiple specimens, and other skull traumas were reasoned to be the result of falling cave-roof pebbles, not flying projectiles.

Many studies were also conducted using primate behavior models, relying on the context of habitat. Baboons, occupying an ecological zone thought to be similar to that of the South African Pleistocene, were used as a model of habitat and adaptive behavior for early hominins. The South African savanna is home to the chacma baboon, a primate with a carnivorous appetite, conclusively deciding for Dart (1957) that australopiths were carnivorous killers. This view was supported by Bartholomew and Birdsell (1953), who speculated early hominids lived on diets similar to baboons consisting of vegetables supplemented by the occasional small animal, Washburn (1957), who related the social consequences of meat-eating (i.e. cooperation, tool use) as predictive factors of becoming human, and Oakley (1961), who felt that apes were vegetarian, while humans and their ancestors were meat-eaters.

Morphological

In 1954, Robinson categorized *Australopithecus africanus* as a meat eater, but based on morphology instead. Moreover, he argued that the teeth alone of *Paranthropus robustus*, *Australopithecus africanus*, and early *Homo* are proof of niche separation despite what at the time were thought to be temporal and geographic overlap. He categorized *Australopithecus africanus*, with its equal anterior and posterior dentition, larger canines, and smaller premolars and molars, as having a nearly

omnivorous diet including fair amounts of meat. *Paranthropus robustus*' massive molars, small anterior dentition, and smaller canines led Robinson to categorize it as having a predominately specialized vegetable-based diet, resulting in its heavy musculature. Early *Homo* was classified as having a totally omnivorous diet, showing dietary competition and consequential displacement was unlikely.

In 1968, Groves and Napier examined incisor to molar row length ratios, noting that specimens with coarser diets consisting of stems, roots, and bark have relatively longer molar row lengths. This placed robustus as having a coarser and "more intensely vegetarian diet" than *Australopithecus africanus*. Jolly (1970) was one of the first to use the morphology of baboons as a model for early hominin diets with the "seed-eater hypothesis." Comparing the gelada baboon, *Theropithecus gelada*, with the genera *Papio* and *Mandrillus* in terms of cranial features and diet, he drew parallels between the primates' differences and the differences found in early hominins. The gelada baboon shares many features with *P. robustus*, including evidence of very powerful masticatory muscles, a more vertical face, and expanded posterior teeth. Jolly considered these cranial features more specialized than that of *Papio* and *Mandrillus*, which represent a more gracile morphology and correspondingly generalized diet. The gelada baboon, with its small incisors and large molars, eats grass seeds collected by hand in the savanna (requiring little incisor processing), leading Jolly to conclude that early hominin incisor reduction (as seen in *P. robustus*) could be attributed to its diet of small tough objects similar to the grass seeds found in the Gelada, as the form of the incisors would be determined by its function (the smallest functional size would be selected for, and lack of alveolar stress would limit space for incisors).

While certainly monumental, Jolly's study had drawbacks, including the fact that grass seeds are seasonal, and earlier hominins (afarensis) have large incisors (Dunbar, 1976). Regardless, this study showed that the highly specialized diet found in the gelada results in similar morphology to the (then considered) highly specialized *P. robustus*, while the generalized diet of *Papio* corresponds to the similar morphology found in *A. africanus*. This gradient compares to the morphology-based niche separation identified by Robinson (1954), and later substantiated by Grine (1981, 1986).

In 2007, Ungar analyzed the surface topography of *P. robustus* and *A. africanus* molars using a laser scanner and geographic information systems (GIS) technology. A laser scanner obtains a three-dimensional point cloud of the surface topography, which is then uploaded to GIS software for analysis.

The software interprets point clouds like landscapes, with cusps treated as mountains, and grooves as valleys, allowing for the use of worn teeth in analyses, unlike former methods (i.e. shearing quotients) (Kay, 1984). Ungar (2007) found the occlusal surfaces of *A. africanus* second molars show more relief than those of *P. robustus*, confirming suggestions *A. africanus* engaged in less grinding and crunching that its robust counterpart.

Dental Microwear

In 1981, Grine published a dental microwear and morphology study of deciduous *A. africanus* and *P. robustus* molars. Using a scanning electron microscope, Grine noted that robust Swartkrans specimens had many pits and dentin islands with steep slopes, indicating a heavier reliance on preparatory "puncture-crushing trituration" than the gracile specimens, which instead had smooth edges around the dentin islands. The robust hominins furthermore had high frequencies of scratches and pitting near cuspal tops, indicating Phase I activities involving more grinding than shearing. When Grine included cusp slope, with *A. africanus* showing more occlusal relief, he concluded that the *P. robustus* dentition was specialized to grind and crush harder and more fibrous foods than *A. africanus.*.

Grine followed this in 1986 with a quantitative dental microwear analysis of adult hominin molars. Again using a scanning electron microscope, Grine used quantifiable measures of scratch and pit direction size, shape and density. He found that P. robustus had a greater number of microwear features and higher incidences of pitting (relative to scratching), with its scratches displaying greater degrees of directional heterogeneity. The pits were also larger in *P. robustus* than *A. africanus*, suggesting to him that the robust hominin dentition was subjected to more hard objects (and consequential crushing and grinding) than the gracile hominins'. He concludes by arguing the dental microwear shows *P. robustus* did not simply process more of the same food items that *A. africanus* encountered, but rather chewed entirely different food items than those triturated by *A. africanus*. This is substantiated by the stark differences in dental proportions and craniomorphology of the two, independent of body size.

While interesting in its results, the methodology, using a scanning electron microscope, posed problems of repeatability and observed results (Grine et al., 2002). Inter-observer error prevented standardized comparisons, as one person may have counted a feature while another may have

overlooked it. In 2003, Ungar et al. proposed a new methodology and analysis protocol to approach these challenges. Using scanning confocal microscopy and scale-sensitive fractal analysis, researchers can compare fossil samples to extant primate data to distinguish among diets by wear patterns based on different fracture properties. The idea of scale-sensitive analysis can be compared to the texture of a surface that changes with the scale of observation; if one were to look at a road, it appears relatively flat from eye level, but with increasing resolution, the road increases in roughness so that it no longer appears smooth and flat, but bumpy. When applied to dental microwear, scale-sensitive fractal analysis measures anisotropy (epLsar - exact proportion length-scale anisotropy of relief), or the directionality of features, and complexity (Asfc – area scale fractal analysis complexity), among other measures like Smc (scale of maximal complexity), HAsfc (heterogeneity of complexity), and Tfv (textural fill volume) (Ungar et al., 2003, Scott et al., 2006).

Using this methodology, Scott et al. (2005) reanalyzed the sample of adult maxillary second molars of *A.* africanus and *P. robustus* originally studied by Grine (1986). The study compared the aforementioned statistics of characteristic primate wear patterns (associated with respective diets) to the 19 fossil specimens. In 1986, Grine found differences between the hominins in relation to pit frequency and heterogeneity, which was supported by Scott et al. (2005). The 2005 study found that *Paranthropus* teeth differed from *Australopithecus* specimens in that they were more complex and more variable in their complexity than *Australopithecus*. Correspondingly, *A. africanus* was found to be more anisotropic and variable in anisotropy than *P. robustus*.

Furthermore, the analysis revealed substantial overlap between the two species in complexity, despite each representing an extreme on opposing ends of the microwear spectrum. This overlap was shown in the greater amount of variation in complexity found in *Paranthropus*, and the greater amount of variation in anisotropy found in *Australopithecus*, suggesting these species changed their diets regularly, but that their preferred resources probably overlapped. The distinctive characteristics exhibited by each species may relate to those critical resources ingested only during parts of the year due to seasonal availability or microhabitat. The findings confirmed that, in reference to extant primates, hard, brittle foods leave more complex textures riddled with pits on tooth surfaces, and tough foods leave more anisotropic

textures with many striations meaning that *A. africanus*, therefore, ate more tough foods and, despite significant dietary overlap, *P. robustus* ate more hard and brittle items.

Materials and Methods

With advances in analytical methodology and technology, studies in relation to both extant and fossil dental microwear have obtained a level of uniformity and definition allowing for a higher resolution of comparison. The introduction of confocal microscopy initiated the production of three-dimensional coordinate scans with associated digital data, allowing for uniform analysis. Researchers are now confident that variation within and between species reflects true variation within that sample instead of noise introduced by interobserver error. The next chapter in innovation involves increasing the resolution of microwear comparison, as introduced by the new instrument.

This study incorporates the use of a new machine, the Plμ Neox Confocal white-light 3D optical profiler (Sensofar Corp.) with a spatial sampling of 0.17μm, and a work envelope of 242 x 181μm with a 100x magnification (6.5 mm working distance and 0.7 numerical aperture) objective. While former studies scanned four adjacent planes obtained with a lateral point spacing of 0.18μm, which are then analyzed separately and their median values used in follow up analyses, this new machine automatically stitches four fields of view with a 10% overlap, changing the work envelope from 276 x 204μm total (or four separately analyzed surfaces of 138 x 102 μm) to 242 x 181 μm. This new instrumentation has a finer resolution than ever before, allowing researchers to develop finer gradients of categorization. Furthermore, the Plμ Standard equipment is beginning to fail, and the Plμ Neox is quickly becoming the new standard, having been adopted by microwear laboratories in Europe, Australia, and here in the United States.

Before studies could proceed, the Plμ Neox had to first be equipped with the appropriate objectives and calibrated to take scans comparable to those of the Plμ Standard confocal microscope using a 100x objective. This was done by repeatedly testing various settings, including intensity and gain of the confocal light source, and threshold value, on a standardized location on a penny (using a scan from the Plμ Standard confocal microscope as a comparison). The resulting optimal settings of the Plμ Neox can be found in Appendix A, and should serve as standard protocol for this laboratory and others.

This stage of the project examined the occlusal wear patterns on the permanent second molars of *Australopithecus* africanus and *Paranthropus* robustus. The second molar was used because this is the tooth observed in past studies and is therefore needed to assure comparability of results (Grine 1986, Scott et al. 2005). A direct comparison of identical scans from the two different instruments consisted of specimens (N=19) from the South African Sterkfontein, Swartkrans, and Kromdraai formations, including Member 4, 1, and 3, respectively.

The occlusal surfaces, after a gentle cleansing with acetone-soaked cotton swabs, were molded with a polyvinylsiloxane dental impression material, President's Jet Regular Body Dental Impression Material (Coltène-Whaledent). The casts were then poured using clear Epotek 501 epoxy resin and hardener (Epoxy Technologies) at the Paleoanthropology Lab, University of Arkansas. After centrifuging any bubbles away from the occlusal surface, the casts were allowed to harden and then removed from the mold for analysis. These steps had already been completed by the time of this project's initiation. Molds were originally collected at the Ditsong Museum of Natural History in Pretoria, South Africa and the University of the Witwatersrand in Johannesburg by Peter Ungar, Fred Grine, and Mark Teaford.

For this stage of the project, maxillary molar enamel facet 9 was examined on each specimen. Facet 9, which is located on the distobuccal aspect of the protocone (mesiolingual cusp), engages in crushing and grinding motions of both vertical and perpendicular movement during so-called "Phase II" activity, making it a standardized location for microwear studies (Grine, 1986; Krueger et al., 2008). The specimens were oriented under the confocal microscope so the mesiodistal axis of the tooth was horizontal to the viewer, and the lingual half placed closest to the viewer.

Each scan from the 2005 (Scott et al.) study was replicated using the Plμ Neox. This was completed by searching the facet until distinctive landmarks could be identified (see Figure 1). The samples were scanned under a 100x objective with a working distance of 6.5 mm and numerical aperture of 0.7. Four adjacent scans were obtained, and digitally "stitched" together with 10% data overlap for the purpose of alignment. The files were saved in .plu format for use in SolarMap Universal version 3.1.10. where each scan was leveled. If dust particles or extraneous adherents were present, the 'erase defects' function was used to erase the offending data points. The resulting files were saved in .sur format for analysis using scale-sensitive fractal analysis software.

a. **b.**

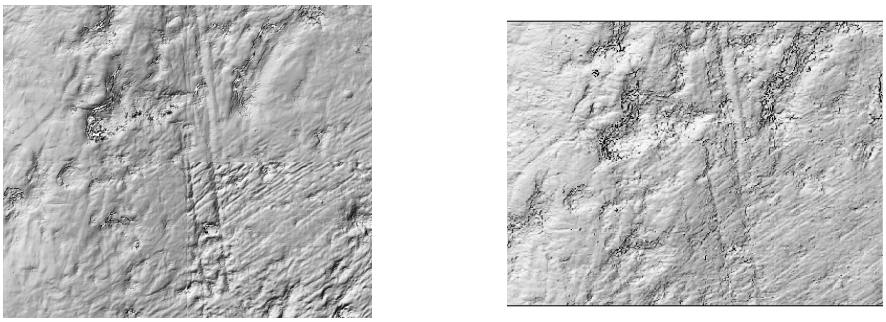

Figure 1. Comparative Scans of SK16 a, b Scan (a.) was taken in 2005, while Scan (b.) was taken in 2014 with the Plμ Neox scanning confocal profiler. Note the different dimensions resulting from the different stitching methodologies. Scan (a.) is a composite image of 4 adjacent, non-overlapping, scans, while Scan (b.), though also a composite image, has a 10% overlap at every border to ensure continuous data.

Once the scan was obtained, the resulting point clouds were processed by Toothfrax and Sfrax programs. These programs have become the standard protocol for many fields, including dental microwear analysis (Ungar et al., 2003; Scott et al., 2005, 2006).

Scale-sensitive fractal analysis results in many measures, each of which offers a component of comparison for gradients of diet. The most frequently used measures to describe teeth are 'anisotropic' (a reflection of epLsar) and 'complex' (a reflection of Asfc).

If a surface is anisotropic, the features exhibit similar directionality, and are visually represented by a rosette with very different lengths. Each vector in a rosette is a cross section taken at the angle in which the vector points. If the surface at that cross section is very bumpy (perhaps perpendicular to many scratches), many points are needed to mark each trough and apex. When these points are connected to one another with lines, and the resulting zig-zag line is straightened, the length will be longer than the cross section's length. If another cross section is taken at the same angle as a scratch, and is therefore entirely within the smooth trough of a scratch, the straightened and flattened cross section, as measured by high and low points, will be much closer to the original length of the cross section. This would be represented by short vector, while a long vector would represent the former surface. Having a rosette with both short and long vectors shows higher directionality because the short vectors will represent the cross sections sitting within the troughs of scratches, while the long vectors will represent the bumpy and variable cross sections taken at angles perpendicular to the features.

Correspondingly, rosettes with vectors of similar length represent low levels of anisotropy, or directionality.

High *epLsar* (anisotropy) has been correlated to the shearing motions associated with folivory. Ungar et al. (2005) found the folivore *Alouatta palliata* to be characterized by a greater degree of, and variance within, anisotropy as compared to the fruit and seed-eating counterpart, *Cebus apella*, which had lower degrees of, and variance within, anisotropy. Foods that leave anisotropic microwear are considered "tough," meaning they are not brittle, but require heavy trituration, characterized by shearing motions, to fragment.

If a surface is complex, there is little uniformity. This is represented by the measurement, *Asfc*, or area-scale fractal complexity. *Asfc* measures the roughness of a relative area by placing triangular patches across the surface, including every peak and pit. That triangulated surface is then measured to find the area, which is then divided by the area of the flat cross-section. The smaller the triangles are, the more precise the complexity. *Asfc* is measured on plots of relative area over scale. As the scale (or size of the triangles) becomes finer, the values for relative area increase. The more complex a surface is, the steeper the slope of the plot becomes when you increase the resolution of triangles. Eventually, though, the triangles become too small to pick up any more detail, which is represented on the plot by a plateau. Where the *Asfc* levels off is called the "scale of maximum complexity," or Smc.

HAsfc measures the heterogeneity of complexity for a surface. By dividing a scan into sub-units of one's discretion (9 cells x 9 cells, 50 cells x 50 cells, etc.), *HAsfc* measures the complexity within each sub-unit and compares them. A homogenous surface would have similar features in each sub-unit, and therefore a low amount of heterogeneity. This type of texture would have a lower HAsfc value than a highly diverse surface where few features are in common between the sub-units.

Textural fill volume (Tfv) measures the number of square cubes, measuring 2μm across on each side, required to fill a surface. Naturally, there are two critical elements: the shape and the texture of the surface. The shape of a surface is measured as Surface fill volume (Sfv), and is in reference to its depth, meaning the total fill volume of a more curved surface will be greater than the Sfv of a planar surface, despite having identical textures. This would be like two bowls of varying depth, but with identical scratches on the bottom. To distinguish the minute features from the overall volume, the size of the

cuboids is reduced from whatever sufficiently course volume was necessary to obtain the surface fill volume, to a smaller measurement along each edge. The smaller cuboids measure the Tfv. The surface fill volume (depth) is then subtracted from the textural fill volume, leaving only a measure of the fine-scale subtleties, much like an impression of the surface's complexity. A higher value of Tfv reflects a very bumpy and complex surface, while a lower value reflects a smoother texture.

Upon acquiring these data for both samples of hominin microwear (those collected on the Plμ Standard, and those collected on the Plμ Neox), a Spearman's Rho correlation test was implemented for both *Asfc* and *epLsar* to assess the significance of correlation between the data gathered on the two confocals. Spearman's Rho was used rather than Pearson's correlation coefficient, because we cannot assume the texture variables are normally distributed. The original study analyzed only *Asfc* and *epLsar* (other measures were not fully developed at the time), guiding the protocol for both Study I and II. A MANOVA on ranked data was used to assess significance of texture variation among the species for the sample obtained using the new Plμ Neox. ANOVAs were carried out for each variable to determine the sources of significant variation between the species. In addition, Bartlett's Tests were used to compare the distributions of *Asfc* and *epLsar* values among taxa.

STUDY II

The purpose of study II is to expand the sample size found in study I in order to independently analyze a sample using the Plμ Neox, and to see if the results corroborate the original findings obtained on both the old and new confocal microscopes. The sample was expanded by including analyses of more *A. africanus* specimens (n=38), including those from members 4 and 5 (dated 2-3 Ma and 2.0-2.6 Ma, respectively) of the Sterkfontein formation (Sterkfontein Witwatersrand) (Moggi-Cecchi et al., 2006), and the Limeworks Dump of the Makapansgat formation, dated at 3.03-2.58 Ma (Herries et al., 2010). A specimen list can be found in Appendix B. The additional specimens were molded by Peter Ungar, Fred Grine, and Mark Teaford at the University of the Witwatersrand in Johannesburg, and casts were prepared as in Study I in the Ungar lab at the University of Arkansas.

Background (see STUDY I: Background)

Materials and Methods

The sample for Study II (N=38) more than triples the size of the original collection of *A. africanus* (N=10), offering greater insight of the variation of this hominin's diet. While the original study used only upper second molars, this expansion included all molars, some of which were mandibular. Each individual is represented by only one dental specimen. Facet 9 was isolated on all specimens, and has been shown to yield no significant differences in mandibular-maxillary comparisons (Teaford and Walker, 1984). The procedure to identify facet 9 on maxillary molars is outlined above. Mandibular facet 9, however, is located on the lingual aspect of the hypocone (distobuccal cusp), and is considered a "Phase II" surface – it comes into direct contact with the opposing facet 9 on the upper molar. Specimens were prepared and scans were obtained using the techniques outlined in Study I, using the settings found in Appendix A. See Appendix B for details on the Study II sample.

Upon gathering scans, the resulting files were edited in SolarMap (Surfract Corp.) and processed through ToothFrax and Sfrax for scale-sensitive fractal analysis (Scott et al. 2006). A MANOVA on ranked data was used to assess significance of texture variation among the species. ANOVAs were carried out for each variable to determine the sources of significant variation between the species. In addition, Bartlett's Tests were used to compare the distributions of *Asfc* and *epLsar* values among taxa.

STUDY III

The purpose of Study III is to generate a sample of extant microwear data using the Plμ Neox. By comparing the data gathered by the Plμ Neox with known dietary strategies of pitheciids, we can assess the efficacy of the instrument and dental microwear texture analysis. This study analyzed the dental microwear of three genera of Pitheciidae, including *Chiropotes*, *Callicebus*, and *Pithecia*.

Background: Pitheciid Diets

Pitheciid diets include a varying amount of unripe fruits with hard pericarps, classifying the group as sclerocarpic foragers, or "predispersal seed predators" (Rosenberger et al. 1996, Norconk et al. 1998). This diet alleviates seasonal pressures, allowing pitheciids to eat even during the dry season, and

reduces competition with sympatric primates. Pitheciids vary in their degree of sclerocarpy, with *Chiropotes* consuming extremely hard-shelled seeds more frequently than *Pithecia*, and *Callicebus* balancing seed intake with a more generic diet of fruits and leaves (Kinzey and Norconk, 1990; Norconk and Conklin-Brittain, 2004; Kinzey, 1997).

Of the genera examined in Study III, *Chiropotes* has the most specialized dental adaptations. Along with robust mandibles and "styliform" incisors (Kinzey, 1992; Rosenberger, 1992; Anapol and Lee, 1994), the canines of these primates are extremely tall and robust. The canines are used to puncture and crush hard seeds (Rosenberger, 1992), while the incisors are used to remove the protective outer layer surrounding the seed. The molars of *Chiropotes* are low, flat, small, and simple (Kinzey, 1992), reflecting the grinding motion required to break down the inner seed.

Pithecia does not bite through pericarps as hard as those found in the diet of *Chiropotes*, but consumes seeds with a higher resistance to crushing than other pitheciines (Kinzey, 1992). *Pithecia* eats few leaves, but more than *Chiropotes* (Kinzey, 1992; Rosenberger et al., 1996). The laterally splayed canines of this primate are used to puncture hard seeds and open fruits. The molars of *Pithecia* are small and low, but show more relief and definition than *Chiropotes*. This is interpreted as an indicator of grinding more pliable seeds than *Chiropotes* (Kinzey, 1992). Dental microwear analyses (using SEM) in a previous study showed that *Pithecia* surface textures had more pits and fewer scratches than found in ripe fruit specialists (Teaford and Runestad, 1992), markers consistent with seed predation.

Callicebus consumes the least sclerocarpic fruit of the three, consuming more fruit flesh than other pitheciines (Kinzey, 1997;, Műller 1996). Consequently, this genus is associated with thin short incisors (Rosenberger, 1992). *Callicebus* has the smallest canines of the three genera, using them for peeling fruit husks and to scrape the mesocarp from hard seeds (Kinzey, 1974, 1977; Rosenberger 1992). While these primates have the smallest canines, they also possess the largest relative molar area (Norconk et al., 2009). These unspecialized surfaces are used for triturating a variety of foods, like fruits, seeds, insects, and leaves.

With their varying levels of sclerocarpy, these genera provide an excellent range of dietary adaptations against which we can compare dental microwear textures obtained with the Plμ Neox confocal profiler.

Materials and Methods

The taxa examined in this study include specimens representing *Ch. satanas* (*n* = 14), *P. irrorata* (*n* = 8), and *Ca. moloch* (*n* = 24) from the Brazilian Amazon (Oriximina, UHE Samuel, and Taperinha, respectively for each of the species). This sample is housed in multiple museums, including the American Museum of Natural History in New York, The National Museum of Natural History in Washington DC, and Goeldi Museum in Belém. Molds were prepared by Peter Ungar and Mark Teaford at each museum, and casts for study were created using epoxy resin and hardener following the procedure outlined above for the early hominin studies.

Epoxy casts of Phase II facets of upper M2s were scanned in blue light using a Plμ Neox scanning confocal profiler (Sensofar Corp.) with a 150x objective (0.3 mm working distance and 0.95 numerical aperture, spatial sampling = 0.11 μm, work envelope = 162 x 121 μm) (for instrument settings, see Appendix A). Resulting point clouds were edited in SensoMap v.6.2 and analyzed using scale-sensitive fractal analysis (Scott et al., 2005). Surface texture complexity (*Asfc*) and anisotropy (*epLsar*) were calculated to characterize each surface.

A MANOVA on ranked data was used to assess significance of texture variation among the species. Single-classification ANOVAs for each variable and Tukey's pairwise HSD tests were then used to identify sources of significant variation as needed. In addition, Bartlett's Tests were used to compare the distributions of *Asfc* and *epLsar* values among taxa, and pairwise two-sample variance tests were used to determine sources of variation as warranted.

RESULTS

Study I

The findings of Study I, which involved scanning the same areas on the hominin molars of the Scott, et al. (2005) sample as closely as possible given the differing work envelopes, showed that, despite using two different machines and areas sampled, the instruments produce results that are significantly correlated for both *Asfc* (fig. 2a) and *epLsar* (fig. 2b) values (n=19). The original study, using the Plμ Standard, found *P.robustus* microwear textures to be significantly more complex (*Asfc* 4.29 ± 2.150; the median and the range) and more variable in complexity than *A. africanus* (*Asfc* 1.686 ± 0.52**),** while *A.*

africanus was found to have surface textures significantly more anisotropic (*epLsar* 0.0045 ± 0.00163) and more variable in anisotropy than *P. robustus* (*epLsar* 0.0028 ± 0.00060) (Scott, et al., 2005). The authors concluded, therefore, that *A. africanus* had a tougher diet, on average, than *P. robustus*, and one that was more variable in its toughness. *P. robustus* was interpreted to have relied upon hard, brittle foods, but the overlap in *Asfc* between the taxa implied that this robust hominin was unlikely to have been a hard-object specialist.

The data gathered on the Plμ Neox for the original sample confirmed the average differences between species (see Table 1a.). One extreme specimen was excluded from the statistical analysis, but is included in Figure 2 for visual reference. *Paranthropus robustus* (*Asfc* 3.171 ± 1.647), again, possessed surface textures found to be significantly more complex (p = 0.014; see Table 1b.) than *A. africanus* (*Asfc* 1.823 ± 1.025), while *A. africanus* (*epLsar* 0.0043 ± 0.0025) had dental microwear that was significantly more anisotropic (p = 0.009)) and more variable in anisotropy (p = 0.045; Bartlett's test) than *P. robustus* (*epLsar* 0.0021 ± 0.0012). While the dispersions of *epLsar* were significantly different by species, the dispersions of *Asfc* were not (p = 0.698) (see fig. 3). Using a Spearman's Rho non-parametric test, the correlations between the old and new *Asfc* values ((ρ_s = 0.56, n=19), and old and new *epLsar* values (ρ_s = 0.78, n = 19) were significant, despite having different trends in variance.

a.

Multivariate Test Statistics				
Statistic	Value	F-ratio	df	p-value
Wilks's Lambda	0.542	6.333	2, 15	0.01
Pillai Trace	0.458	6.333	2, 15	0.01
Hotelling-Lawley Trace	0.844	6.333	2, 15	0.01

b.

Univariate F Tests					
Source	Type III SS	df	Mean Squares	F-ratio	p-value
ASFC	156.056	1	156.056	7.602	0.014
Error	328.444	16	20.528		
LSAR	193.389	1	193.389	8.835	0.009
Error	350.222	16	21.889		

Table 1. Summary statistics of original sample obtained on the Plμ Neox. a, b, Multivariate statistics (a.) indicating significant difference between the taxa, and F-tests (b.) indicating significant median differences in both *Asfc* and *epLsar*.

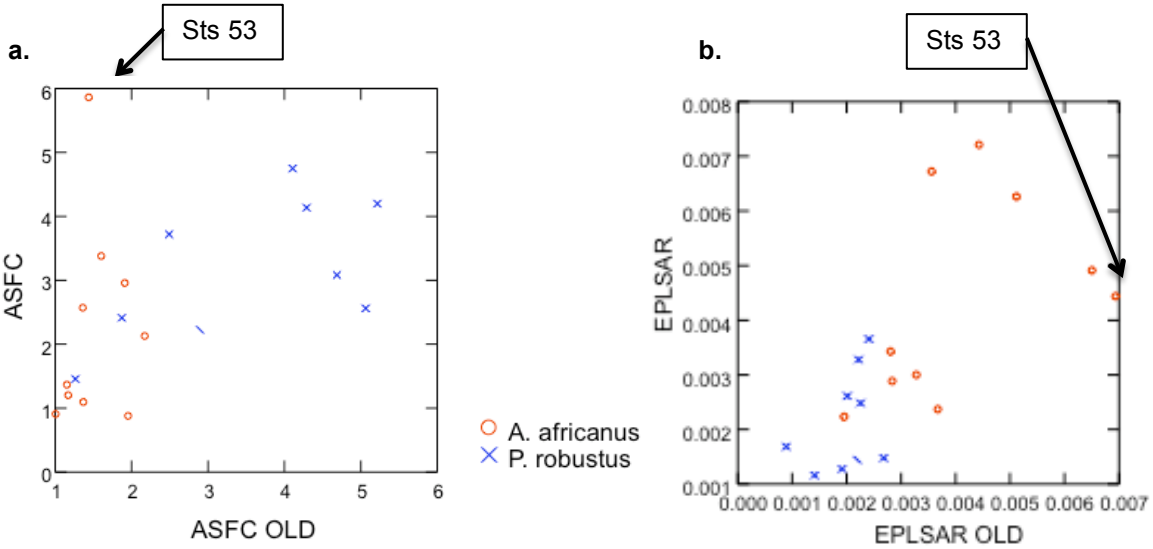

Figure 2. Confocal comparison. a, b, Univariate plots of values obtained from the Plμ Standard (x-axis) versus the Plμ Neox (y-axis) for **(a)** *Asfc* and **(b)** *epLsar*.

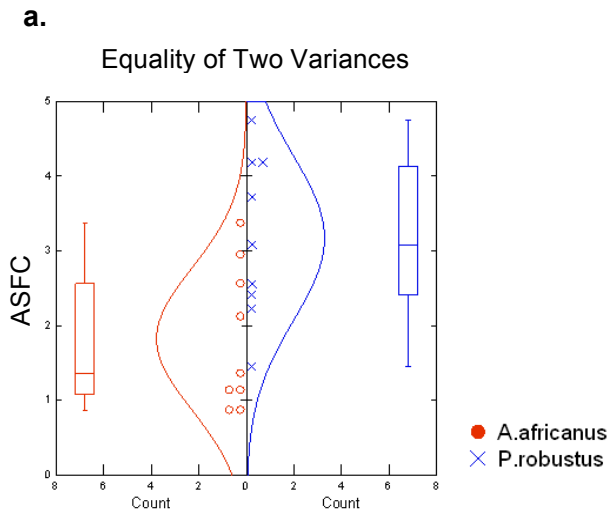

95.00% Confidence Interval	0.17	to	3.34
F-ratio	0.753		
df	8, 8		
p-value	0.698		

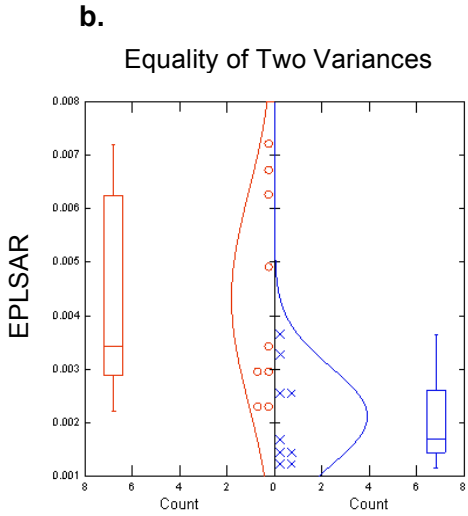

95.00% Confidence Interval	1.036	to	20.37
F-ratio	4.594		
df	8, 8		
p-value	0.045		

Figure 3. Pairwise Two-Sample Variance. a, b, Comparative plots (and p-values) of both *Asfc* (a.) and *epLsar* (b.) variance in the original sample of *A. africanus* and *P. robustus* obtained on the Plμ Neox.

Study II

The expansion of the sample to include more *A. africanus* specimens corroborated some findings of the original study (fig. 4). Combined with the Plμ Neox sample from Study I, *A. africanus* (*Asfc* 1.208 ± 0.889) was consistently found to be significantly less complex ($p < .01$; table 2b) and less variable in complexity ($P = 0.011$) than *P. robustus* (*Asfc* 3.171 ± 1.647), and consistently more anisotropic (*epLsar* 0.0034 ± 0.0069; $p = 0.024$) than *P. robustus* (*epLsar* 0.0021 ± 0.0013) (fig. 5). Interestingly, the different dispersions of *epLsar* values between the taxa were not significant, while the *Asfc* dispersions were (fig. 6). The taxa remain significantly different in median values of both *Asfc* ($p < 0.01$) and *epLsar* ($p = 0.024$) (table 2), but the differences in variation are discordant with the results of Study I.

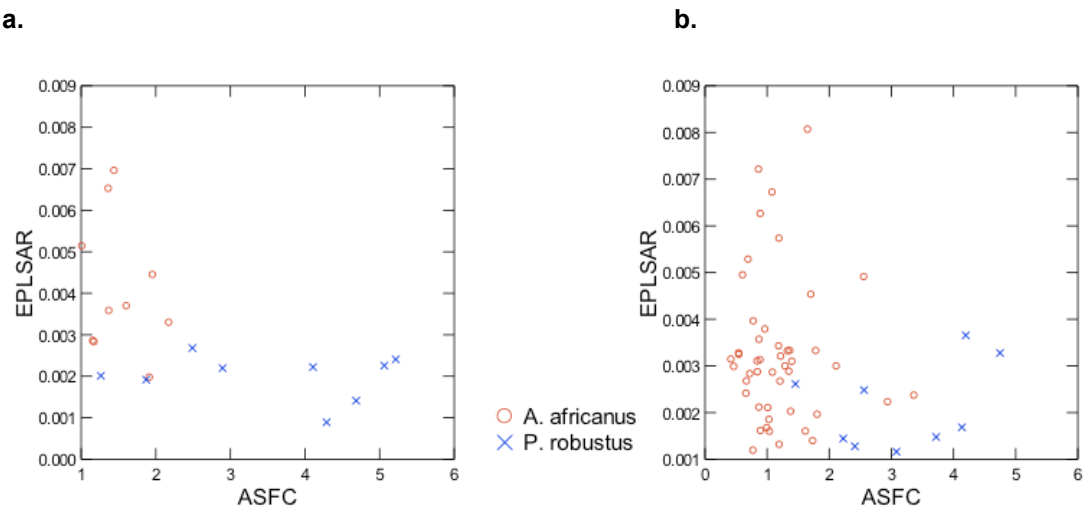

Figure 4. Anisotropy and complexity. a, b, Bivariate plots of *epLsar* versus *Asfc* for *Australopithecus africanus* and *Paranthropus robustus* **(a)** scanned on the Plμ Standard machine **(b).** scanned on the Plμ Neox with the expanded Study II sample.

a. **b.**

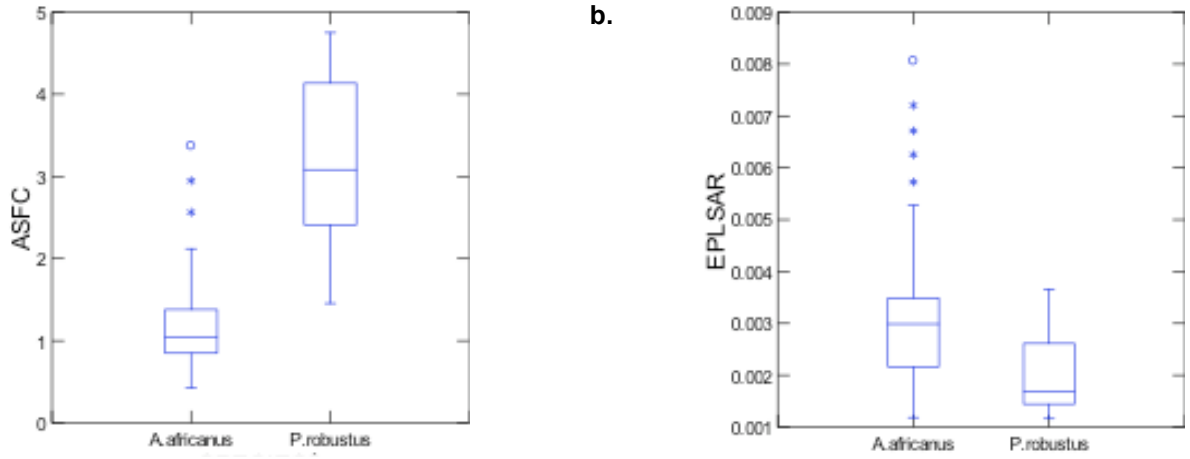

Figure 5. Variation by Species. a, b Plots of **(a)** *Asfc* and **(b)** *epLsar* values versus species (*A. africanus* and *P. robustus*), indicating within-species variation.

a.

Multivariate Test Statistics				
Statistic	Value	F-ratio	df	p-value
Wilks's Lambda	0.545	6.824	6, 49	0.000
Pillai Trace	0.455	6.824	6, 49	0.000
Hotelling-Lawley Trace	0.836	6.824	6, 49	0.000

b.

Univariate F Tests					
Source	Type III SS	df	Mean Squares	F-ratio	p-value
ASFC	4854.955	1	4854.955	26.820	0.000
Error	9775.045	54	181.019		
EPLSAR	1337.149	1	1337.149	5.432	0.024
Error	13292.851	54	246.164		
SMC	2220.175	1	2220.175	9.661	0.003
Error	12409.825	54	229.812		
TFV	407.787	1	407.787	1.548	0.219
Error	14222.213	54	263.374		
HASFC9	857.905	1	857.905	3.364	0.072
Error	13772.095	54	255.039		
HASFC81	1036.894	1	1036.894	4.119	0.047
Error	13593.106	54	251.724		

Table 2. Summary statistics of expanded sample obtained on the Plμ Neox. a,b, Multivariate statistics (a.) indicating a significant difference between the taxa, and Univariate statistics (b.) indicating significant differences in the median values of both *Asfc* and *epLsar* between *A. africanus* and *P. robustus*. Other variables were not considered, following protocol of the original study, however, the other significant measures are *Smc* and *HAsfc81*.

a.

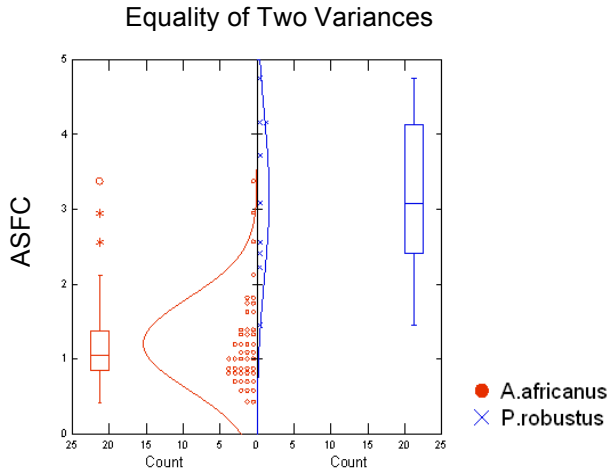

95.00% Confidence Interval	0.081	to	0.768
F-ratio	0.309		
df	46, 8		
p-value	0.011		

b.

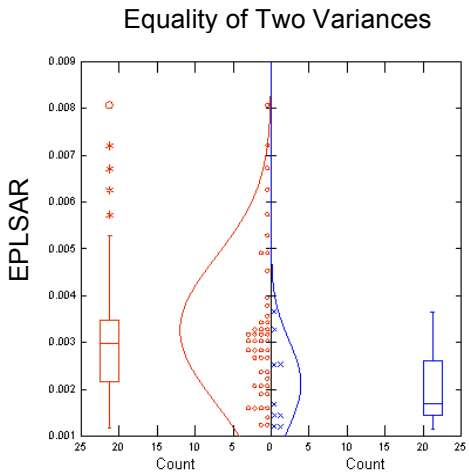

95.00% Confidence Interval	0.758	to	7.18
F-ratio	2.893		
df	46, 8		
p-value	0.114		

Figure 6. Pairwise Two-Sample Variance. a, b, Comparative plots (and p-values) of both *Asfc* (a.) and *epLsar* (b.) of the variance of the expanded sample of *A. africanus* and *P. robustus* obtained on the Plμ Neox

Study III

Statistical analyses showed the pitheciid species did not differ significantly in *Asfc,* but did in *epLsar* ($p = 0.046$), with *Chiropotes satanas'* values significantly lower than that of *Pithecia irrorata* ($p = 0.036$) (fig. 7). The species also differed in their variance of both *Asfc* and *epLsar* values (fig.9). *Callicebus moloch* and *Chiropotes satanas* both had significantly more dispersion in *epLsar* values than did *Pithecia irrorata* ($p < 0.01$ in both instances). *Chiropotes satanas* also had significantly more dispersion in its *Asfc* values than did either *Callicebus moloch* or *Pithecia irrorata* (($p < 0.01$ in both instances).

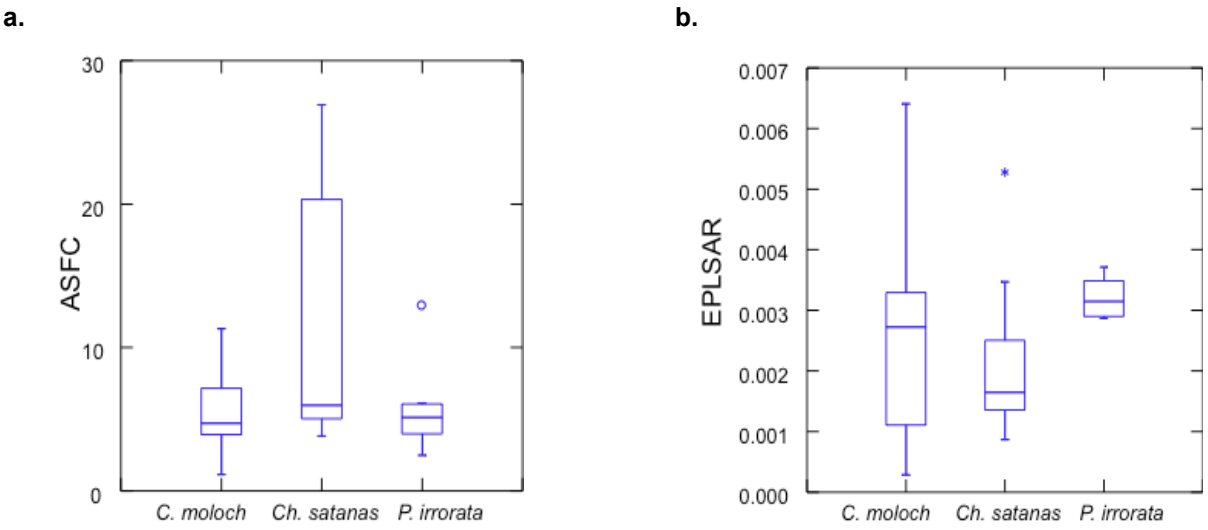

Figure 7. Box Plots a, b Box plots by species of (a.) *Asfc* and (b.) *epLsar*, reflecting median values and within-species variation.

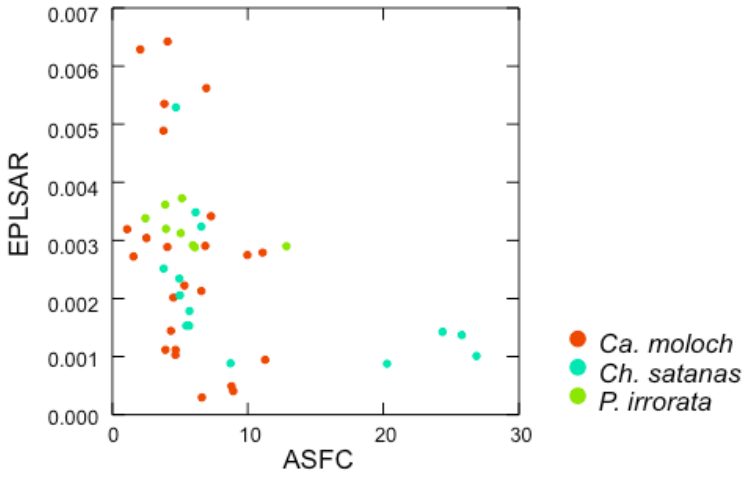

Figure 8. Anisotropy and Complexity Bivariate plot of *Asfc* versus *epLsar* for all species

Univariate F Tests					
Source	Type III SS	df	Mean Squares	F-ratio	p-value
ASFC	726	2	363	2.115	0.133
Error	7381.5	43	171.663		
EPLSAR	1083.863	2	541.932	3.318	0.046
Error	7023.637	43	163.34		

Table 3. Univariate F Tests indicating significant differences in *epLsar* between the three species.

Tukey's Honestly-Significant-Difference Test					
SPECIES	SPECIES	Difference	p-value	95.0% Confidence Interval	
				Lower	Upper
Ca. moloch	Ch. satanas	4.595	0.538	-5.838	15.029
Ca. moloch	P. irrorata	-9.958	0.149	-22.624	2.708
Ch. satanas	**P. irrorata**	**-14.554**	**0.036**	-28.304	-0.803

Table 4. Tukey's HSD Test, which shows the significance in *epLsar* (table 2) lies between *Ch. satanas* and *P. irrorata*.

a.

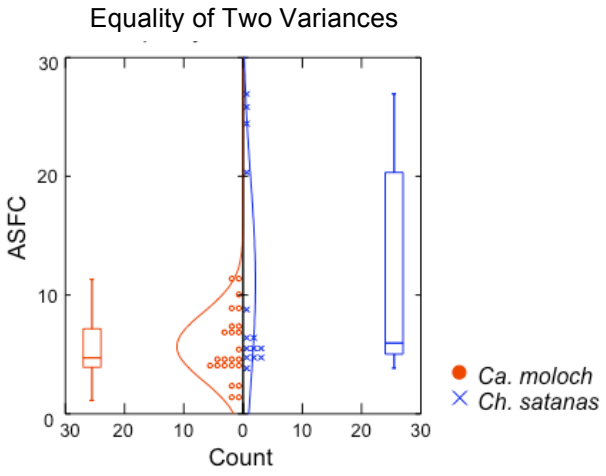

95.00% Confidence Interval	0.035	to	0.259
F-ratio	0.103		
df	23, 13		
p-value	0		

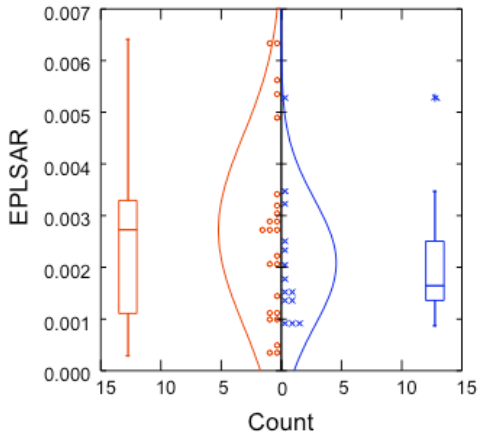

95.00% Confidence Interval	0.772	to	5.68
F-ratio	2.244		
df	23, 13		
p-value	0.133		

b.

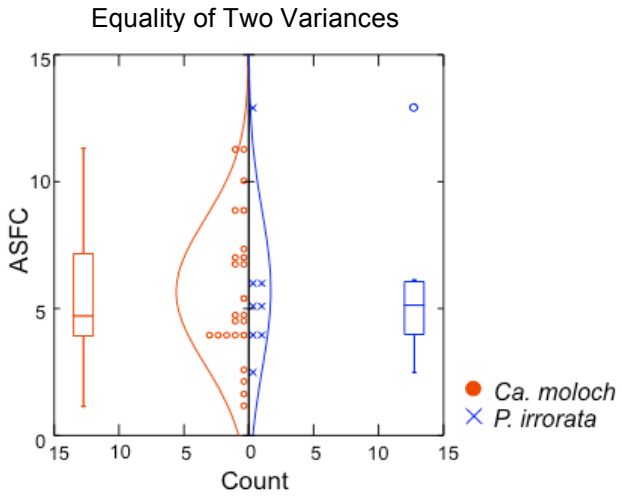

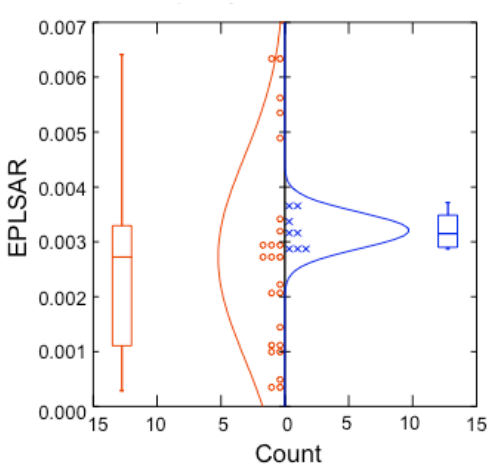

95.00% Confidence Interval	0.188	to	2.409
F-ratio	0.83		
df	23, 7		
p-value	0.679		

95.00% Confidence Interval	7.06	to	90.65
F-ratio	31.2		
df	23, 7		
p-value	0		

c.

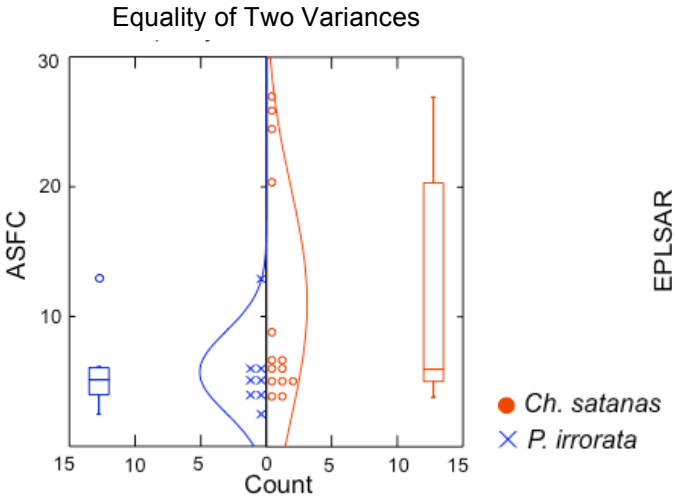

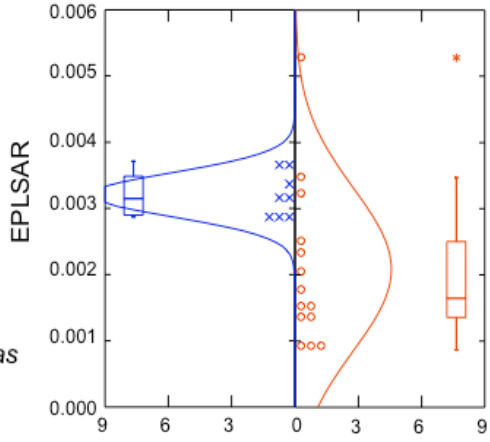

95.00% Confidence Interval	1.749	to	28.197
F-ratio	8.096		
df	13, 7		
p-value	0.01		

95.00% Confidence Interval	3.007	to	48.48
F-ratio	13.91		
df	13, 7		
p-value	0.002		

Figure 9. Pairwise Two-sample Variance a, b, c Comparative plots and significance charts of both *Asfc* (left) and *epLsar* (right) of the variance between (a.) *Ca. moloch* and *Ch. satanas*, (b.) *Ca. moloch* and *P. irrorata*, and (c.) *Ch. satanas and P. irrorata.*

DISCUSSION

Study I, II, and III

Study I, the purpose of which was to compare data from the old and new confocal profilers, found relatively consistent results. The different spatial sampling and different sizes, particularly, of the work envelopes naturally yielded different values between the two machines; the general trends in median values, though, are the same, and the significant correlation between the two machines' data means there are many signals lending confidence to the adoption of the Plμ Neox as a standard for the field. Despite these similar signals, however, the Plμ Neox did not successfully replicate the original study in every dimension.

The challenges of this stage of experimentation included the different work envelope areas and the difficulty of searching for precisely matched areas. The procedures for working on the Plμ Neox initially involved duplicating the procedures required for the Plμ Standard confocal, which included scanning a 2x2 rectangle and stitching them together. Only later did it become apparent that the Plμ Neox overlaps 10% of the each image for the sake of data continuity, which alters the workspace. While scanning a 2x2 image includes a comparable number of measured points to a composite scan from the Plμ Standard instrument, the smaller workspace means less of a sampled area, perhaps affecting results. Furthermore, the old technique of processing each quarter of the total scan separately and then computing the medians tended to homogenize areas and minimize extreme values and outliers that are more likely to be included in the analysis of the Plμ Neox's scans. Scanning a 3x3 rectangle and then cropping out any unnecessary data could have corrected the problem of incongruent areas, but the resulting scans would have discrepant amounts of measured points.

Despite repeatability (or more accurately, the reduction of observer measurement error by eliminating the need to identify and measure all individual features with a mouse-driven pointer) being a major advantage of confocal microscopy over SEM, actually finding/revisiting identical areas on a tooth can prove very difficult, especially when no key landmarks are present. Relatively consistent sites were found for seventeen of nineteen specimens, but the same exact areas could not be identified for two. The original scans of STS 31 and SK49 included landmarks that could not be located again. Perhaps the

original study oriented these two specimens differently, or scanned a portion of an adjacent facet by mistake. Regardless, for these two scans, comparable images were scanned instead with similar, but not identical, features present. The setbacks of this study certainly had a minor bearing on the results, perhaps resulting the lack of significant variation in the Plμ Neox's *Asfc* values, yet the data still generally corroborate those of the original study.

Study II of this experimental trilogy expanded the existing sample of *A. africanus*, and yielded interesting results that did not align with the findings from Study I in terms of variance. While the larger sample saw significant median differences in *Asfc* and *epLsar* between species, the dispersion of values only showed significance in comparing *Asfc* values. This lack of *epLsar* significance could perhaps be explained by the increased sample of values closer to the *Paranthropus* mean identified in (Scott, et al., 2005). Further study, including augmentation of the *Paranthropus* sample to include SKx specimens from Swartkans and the Drimolen sample, is planned. This will result in a more balanced model with comparable sample sizes for the two hominin species.

The overlap in *Asfc* between the two hominins in the original study implied to researchers that *P. robustus* was unlikely to have been a specialized hard-object feeder, like its anatomy would suggest. Instead, they concluded that brittle and hard foods were only an occasional food source, but perhaps important component for survival. Forty-seven percent of the original *Asfc* values overlapped between the species. As the sample increased from n = 19 to n = 57, this overlap decreased to thirty-two percent. This overlap may have decreased, but the conclusion of *P. robustus* being a dietary generalist over a dietary specialist remains, as the heavily weighted *A. africanus* sample naturally increases in range, and decreases the proportion of overlap between species. The overlap may be due to commonly preferred foods, but a reliance on different fallback resources consumed only periodically, perhaps in relation to microhabitat or seasonality (Scott et al., 2005) accounts for the clear differences between taxa. Again, expansion of the sample of *P. robustus* to include the SKx and Drimolen samples will help balance numbers of specimens between the taxa and clarify differences.

Study III examines the dental microwear textures of pitheciids with known dietary behaviors using a 150x objective on the Plμ Neox. Comparisons of median values for complexity and anisotropy were complicated by significant variation in the texture variables, specifically high variation in *Ch. satanas* (in

both complexity/*Asfc* and anisotropy/*epLsar*) and in *Ca. moloch* (in *epLsar*). Still, higher anisotropy in *P.irrorata* compared with *Ch. satanas* may relate to reliance on more tough leaves (and thus more precise masticatory movements) by *P.irrorata* (Mellett, 1985; Kinzey, 1992; Rosenberger et al., 1996; Evans and Sanson, 2006). Although *Ca. moloch* eats more leaves than pitheciines, it is considered a fruit-heavy dietary generalist, and that, plus its smaller canines (and thus perhaps less canine guidance in mastication (Mills, 1963), an area of exploration for future studies) may account for its high variation in *epLsar* (Müller, 1996). The higher dispersion in *Asfc* values for *Ch. satanas* may, in turn, be due to the wider range of material properties of the foods in its diet, as it relies upon the most immature hard seed species of the examined taxa (Kinzey and Norconk, 1990; Müller, 1996; Norconk and Conklin-Brittain, 2004), albeit with significant overlap with *P. irrorata.*

While these results were obtained through analyses of specimens from different museums and different sites of collection in the Brazilian rainforest, they still fell in line with some dietary differences reported in the literature. We expect that better control over sites and dates of capture, and larger samples (*particularly* for *P. irrorata)* will provide more detail on how microwear texture differences relate to diet in these taxa.

CONCLUSIONS

The goals of these studies were to investigate comparability between two scanning confocal microscopes, expand the sample of *A. africanus* microwear texture data, and conduct the first microwear texture analysis of the pitheciids (and in fact, the first such study using primates as small as *Callicebus*). In Study I, the two instruments yielded relatively similar results, despite many limitations including work envelope area incomparability, spatial sampling differences, and specimens whose exact same areas were not replicated. While these results were similar, they only broadly replicated the general trends, meaning there are still efforts to be made in truly replicating an existing study. With the many different features between instruments, however, this may not be possible or even preferable.

Expanding the sample confirmed the original study's general trends, adding confidence in data collected using the new Plμ Neox confocal profiler, however, there were still trends in variance that did not correspond to the original results. Using a sample of pitheciid primates in Study III, the Plμ Neox

proved capable of generally parsing species with reported differences in diet in predictable ways, lending evidence toward the efficacy of the new instrument. There were some unexpected results, but accounting for season of collection and sample size in the future might lead to results more in line with predicted patterning.

This study also led to insight into primate diets, examining an expanded sample of hominins, and quantifying the dental microwear of previously unexamined pitheciids. *Australopithecus africanus* and *P. robustus* were shown to have triturated significantly different types of foods, regardless of instrument generation, and the hypothesis of *P. robustus* being a dietary generalist was maintained despite a directional sample increase. Observable diets were also generally confirmed by this study, with microwear patterns of pitheciid diets by taxa broadly conforming to documented dietary specialization.

The generalized success of the new instrument in each stage implies that with future studies and experimentation, the Plμ Neox may become an effective instrument for the quantitative characterization and comparison of dental microwear textures to be utilized in laboratories around the world.

APPENDIX A

Using the 100x Objective:

The following outlines the standard settings when using a 100x objective on the Plμ Neox. After arranging one's specimen and preparing an area to scan, the field of view must be changed to "Confocal" mode. Make sure the <OBJECTIVE is set to 100x. If stitching multiple areas together, "Extended Topography" must be selected under the <MEASUREMENT menu. The "THRESHOLD" must be set at 1.5%. Under the <LIGHT SOURCE menu, the "Confocal Image Gain" setting for "Gain" must be set to 25% in order to obtain optimal scans while the "B&W Camera" and "Color Camera" will remain on default. The setting for "Gamma" will correct itself upon an autofocus of the light. White-light must be selected in confocal mode when scanning under 100x magnification.

Using the 150x Objective:

The following outlines the standard settings when using a 150x objective on the Plμ Neox. After arranging one's specimen and preparing an area to scan, the field of view must be changed to "Confocal" mode. Make sure the <OBJECTIVE is set to 150x. If stitching multiple areas together, "Extended Topography" must be selected under the <MEASUREMENT menu. The "THRESHOLD" must be set at 1%. Under the <LIGHT SOURCE menu, the "Confocal Image Gain" setting for "Gain" must be set to 100% in order to obtain optimal scans while the "B&W Camera" and "Color Camera" will remain on default. The setting for "Gamma" will correct itself upon an autofocus of the light. Blue-light must be selected in confocal mode when scanning under 150x magnification.

APPENDIX B

SPECIMEN	TOOTH*	PHOTO SIMULATION
STW1	LM_1	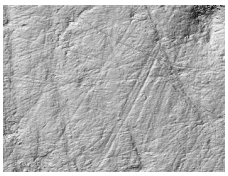
STW11	RM^3	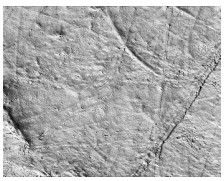
STW13	LM^3	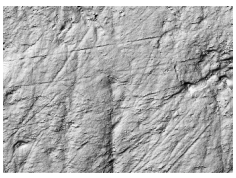
STW34	LM^2	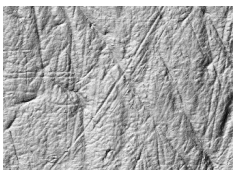
STW37	LM^3	
STW43	RM^3	
STW53	RM^2	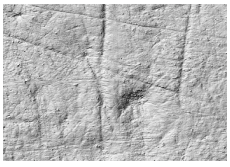
STW61	RM_2	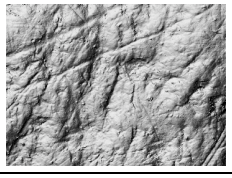

STW71	RM^2	
STW96	LM_3	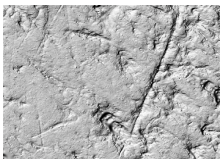
STW131	RM_1	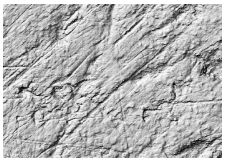
STW134	LM_2	
STW140	LM^3	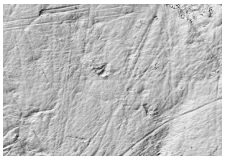
STW183	LM^2	
STW193	LM_2	
STW212	LM_2	

STW220	RM_1	
STW237	LM_3	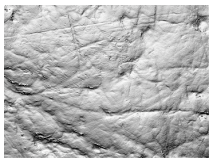
STW252	LM^2	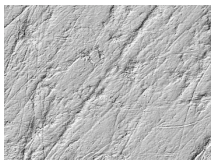
STW291	RM_1	
STW309	RM_1	
STW313	LM_3	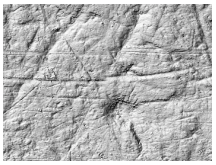
STW353	RM_3	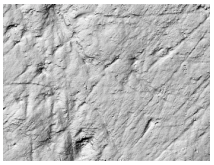
STW397	RM_3	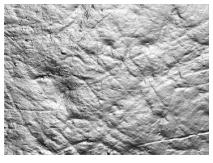

STW404	RM_2	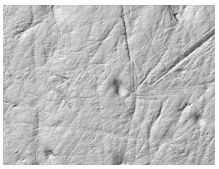
STW421	RM_1	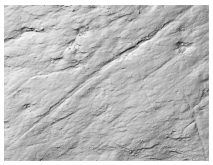
STW450	RM^1	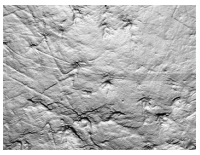
STW487	RM_3	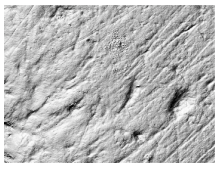
STW498	RM_2	
STW520	RM_3	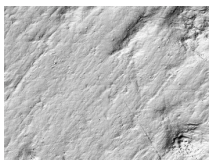
STW524	RM^3	
TM1511	LM^2	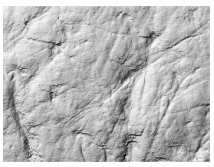

MLD2	LM_2	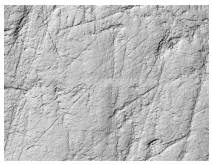
MLD6	RM^2	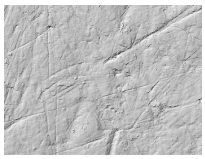
MLD19	LM_3	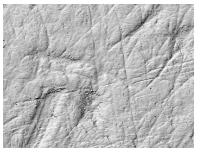
MLD24	LM_1	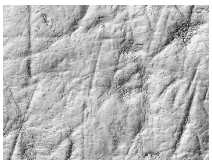
MLD28	RM^3	
MLD44	LM^3	

*All STW specimens identified in Moggi-Cecchi et al. (2006) and MLD specimens identified in Bone and Dart (1955).

REFERENCES CITED

Anapol, F. and Lee, S. 1994. Morphological adaptation to diet in platyrrhine primates. Am. J. Phys. Anthropol. 94:239–261.

Bartholomew, GA and Birdsell B. I953. Ecology and the protohominids. Am. Anthrop. 55:48I-98.

Bone, EL and Dart, RA. 1955. A catalogue of Australopithecine fossils found at the Limeworks, Makapansgat. Am. J. Phys. Anthropol. 13:621-4.

Brain, CK. 1970. New Finds at the Swartkrans Australopithecine Site. Nature 225:1112–1119.

Brain, CK. 1981. *The Hunters or the Hunted?* Chicago: University of Chicago Press.

Dart, RA. 1926. Taungs and its significance. Natural History 26:315-27.

Dart, RA. 1940. Recent Discoveries Bearing on Human History in Southern Africa. The Journal of the Royal Anthropological Institute of Great Britain and Ireland 70:13–27.

Dart, RA. The Makapansgat proto-human Australopithecus Prometheus. Am. J. Phys. Anthropol. 6:259-83.

Dart, RA. 1949. The predatory implemental technique of Australopithecus. Am. J. Phys. Anthropol. 7(1):1-38.

Dart, RA. 1953. The Predatory Transition from Ape to Man. International Anthropological and Linguistic Review 1(4):201-217.

Dart, RA. 1957. The osteodontokeratic culture of Australopithecus prometheus, Transvaal Museum Memoir No. 10. Transvaal Museum, Pretoria

Dunbar, RIM. 1976. Australopithecine diet based on a baboon analogy. Journal of Human Evolution 5(2):161-167.

Evans, AR. and Sanson, GD. 2006. Spatial and functional modeling of carnivore and insectivore molariform teeth. J Morph 267:649–662.

Grine, FE. 1981. Trophic differences between ‘gracile’ and ‘ro- bust’ australopithecines: a scanning electron microscope analysis of occlusal events. S Afr J Sci 77:203–230.

Grine, FE. 1986. Dental evidence for dietary differences in Australopithecus and Paranthropus: a quantitative analysis of permanent molar microwear. J Hum Evol 15:783–822.

Grine, FE., Ungar, PS., Teaford, MF. 2002. Error rates in buccal-dental microwear quantification using scanning electron microscopy. Scanning 24:144-153.

Groves, CP. and Napier, JR. 1968. Dental dimensions and diet in australopithecines. Proc. VIII Int. Cong. Anthrop. Ethnological Science 3,:273–276.

Herries, A., Hopley, P., Adams, J. 2010. Letter to the editor: Geochronology and palaeoenvironments of South African hominin-bearing localities—A reply to Wrangham et al., 2009. “Shallow-Water Habitats as Sources of Fallback Foods for Hominins.” Am. J. Phys. Anthropol. 143(4):640-6.

Jolly, C. 1970. The Seed-Eaters : A New Model of Hominid Differentiation Based on a Baboon Analogy. Man 5:5–26.

Kay, RF. 1984. On the use of anatomical features to infer foraging behavior in extinct primates. In: Rodman, (PS., Cant, JGH. Eds), Adaptations for Foraging in Nonhuman Primates: Contributions to an Organismal Biology of Prosimians, Monkeys and Apes. Columbia University Press, New York, pp.21-53.

Krueger, KL., Scott, JR., Kay, RF., Ungar, PS. 2008. Technical Note: Dental Microwear Textures of "Phase I" and "Phase II" Facets. Am. J. Phys. Anthropol. 137:485-490.

Kinzey, WG. 1974. Ceboid models for the evolution of hominoid dentition. J. Hum. Evol. 3:193–203.

Kinzey, WG. 1977. Diet and feeding behavior of *Callicebus torquatus*. In (T.H. Clutton-Brock ed.) Primate Ecology: Studies of feeding and ranging behaviour in lemurs, monkeys and apes, pp. 127–151. London: Academic Press

Kinzey, WG. 1992. Dietary and dental adaptations in the Pitheciinae. Am. J. Phys. Anthropol. 88:499–514.

Kinzey. WG. 1997. *Callicebus*. In (W.G. Kinzey ed) New World Primates: Ecology, evolution, and behavior, pp. 213–221. New York: Aldine de Gruyter.

Kinzey, WG. and Norconk, MA. 1990. Hardness as a basis of fruit choice in two sympatric primates. Am. J. Phys. Anthropol. 81:5-15.

Mellett, JS. 1985. Autocclusal mechanisms in the carnivore dentition. Aust Mammal 8:233–238.

Mills, J. R. E. I963. Occlusion and malocclusion in primates. In Dental anthropology (ed.) D. R. Brothwell. Oxford: Pergamon Press.

Moggi-Cecchi, J., Grine, FE., Tobias, P. 2006. Early hominid dental remains from members 4 and 5 of the Sterkfontein Formation (1966-1996 excavations): catalog, individual associations, morphological diescriptions and intial metric analysis. J. of Hum. Evol. 50(3):239-328.

Müller, KH. 1996. Diet and feeding ecology of masked titis (*Callicebus personatus*). In (M.A. Norconk, A.L. Rosenberger, P.A. Garber eds) Adaptive Radiations of Neotropical Primates, pp. 383–401. New York: Plenum Press.

Norconk, MA., Grafton, BW., Conklin-Brittain, NL. 1998. Seed dispersal by Neotropical seed predators. Am. J. Primatol. 45:103–126.

Norconk, MA., Conklin-Brittain, N. 2004. Variation on Frugivory: The Diet of Venezuelan White-Faced Sakis. International Journal of Primatology 25(1):1-26.

Norconk, MA., Wright, BW., Conklin-Brittain, NL., Vinyard, CJ. 2009. Mechanical and Nutritional Properties of foods as factors in Platyrrhine dietary adaptations. In (PA. Garber, A. Estrada, JC. Bicca-Marques, EW. Heymann, KB. Strier eds) South American Primates: Comparative Perspectives in the Study of Behavior, Ecology, and Conservation, pp. 279–319. Springer Science.

Oakley, KP. 1961. On man's use of fire, with comments on tool-making and hunting. Social life of early man 31:176-193.

Robinson, JT. 1954. The genera and species of the Australopithecinae. Am J Phys Anthropol 12:181–200.

Rosenberger, AL. (1992). Evolution of feeding niches in New World Primates. Am. J. Phys. Anthropol. 88, 525–562.

Rosenberger, AL., Norconk, MA., Garber, PA. 1996. New perspectives on pitheciines. In (M.A. Norconk, A.L. Rosenberger, P.A. Garber eds) Adaptive Radiations of Neotropical Primates, pp. 329–334. New York: Plenum Press.

Scott, RS., Ungar, PS., Bergstrom, TS., Brown, CA., Grine, FE., Teaford, MF., Walker, A. 2005. Dental microwear texture analysis shows within-species diet variability in fossil hominins. Nature 436:693–5.

Scott, RS., Ungar, PS., Bergstrom, TS., Brown, CA., Childs, BE., Teaford, MF., Walker, A. 2006. Dental microwear texture analysis: technical considerations. Journal of Human Evolution 51:339–49.

Teaford, MF and Runestad, JA. 1992. Dental microwear and diet in Venezuelan primates. Am. J. Phys. Anthropol. 88(3):347-364).

Ungar, PS., M'Kirera, F. 2003. A solution to the worn tooth conundrum in primate functional anatomy. Proceedings of the National Academy of Sciences of the United States of America [Internet] 100:3874–7.

Ungar, PS., Brown, CA., Bergstrom, TS., Walker, A. 2003. Quantification of dental microwear by tandem scanning confocal microscopy and scale-sensitive fractal analyses. Scanning 25:185–93.

Ungar, PS. 2005. Reproductive fitness and tooth wear: Milking as much as possible out of dental topographic analysis. Proceedings of the National Academy of Sciences of the United States of America 102:16533–16534.

Walker, A. and Teaford, MF. 1984. Quantitative Differences in Dental Microwear Between Primate Species With Different Diets and a Comment on the Presumed Diet of Sivapithecus. Am. J. Phys. Anthropol. 64:191-200.

Washburn, SL. 1957. Australopithecines: the hunters or the hunted? *American Anthropologist 59*(4):612-614.